Electronic Supplementary Material (ESI) for CrystEngComm.

Supporting Information

1. Materials and instruments

1.1 Materials

$Y(CH_3COOH)_3{\cdot}4H_2O$, $Yb(CH_3COOH)_3{\cdot}4H_2O$, $Tm(CH_3COOH)_3{\cdot}4H_2O$, $Gd(CH_3COOH)_3{\cdot}4H_2O$, oleic acid, 1-octadecene, and polyvinylpyrrolidone (Mw=40,000) were purchased from Sigma-Aldrich. 1,4-benzoquinone, ethylenediaminetetraacetate, and 2-aminoterephthalic acid, and Rhodamine B were purchased from Adamas. NaOH, NH_4F, Chromium nitrate nonahydrate and isopropanol were purchased from Greagent. All the chemical reagents were used as received without further purification.

1.2 Experimental and characterization instruments

The microstructure of NYT, NYTG(3%), and NYTG(3%)/NMC were studied by a transmission electron microscope (TEM, JEM-2100, operated at 200 kV). The crystal structures of all the samples were analyzed by the X-ray diffraction instrument (XRD, Bruker D8 Advance) with a Cu Kα radiation source (λ = 0.15418 nm) operated at 40 kV and 40 mA. The UV-Vis-NIR diffuse reflectance spectra (DRS) of the as-prepared solid samples were investigated by using a PE Lambda 950 spectrophotometer, which equipped with an integrating sphere. The upconversion luminescence spectra were obtained by using a Fluorescence spectra were recorded on FluoroMax+ spectrometer with an external 980 nm NIR laser. The XPS spectra were performed by Thermo Scientific K-α + XPS spectrometer with the monochromatized Al-Kα X-ray source (hν = 1486.8 eV). The 400 μm X-ray spot was used for XPS analysis. The absorbance of RhB in aqueous solutions was measured using a UH4150 spectrophotometer. Photocatalytic efficiency of RhB decomposition was tested under UV-Visible (<760 nm), near–infrared light (>760 nm) and full−spectra−light irradiation with a 300 W Xenon lamp (Perfect Light PLS-SXE-300+) that equipped with a cooling system for temperature control. The simulated solar light photocatalysis reaction was carried out using a solar simulator (AM 1.5 G).

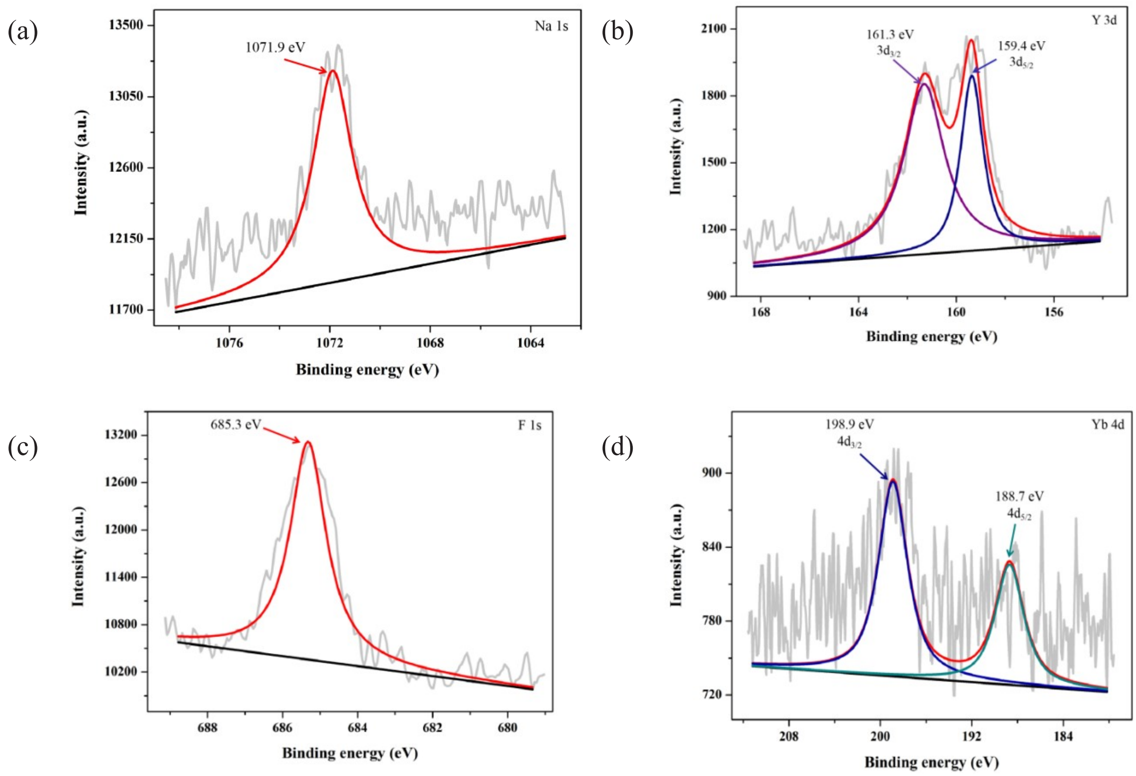

Fig. S1. XPS spectra of NYTG(3%)/NMC: (a) Na 1s, (b) Y 3d, (c) F 1s, and (d) Yb 4d

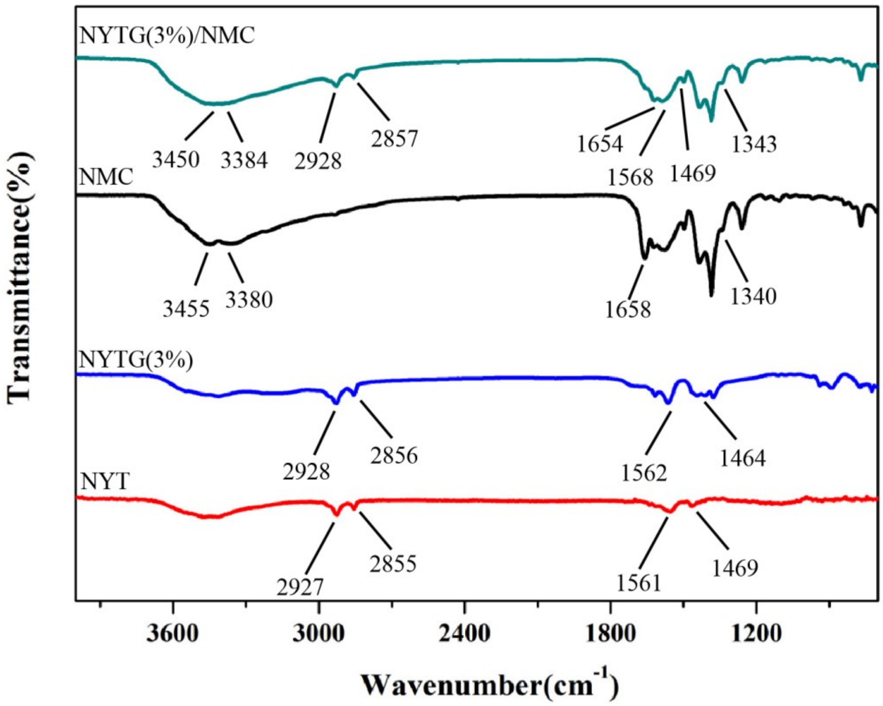

Fig. S2. Fourier transform infrared (FTIR) spectra of NYT, NYTG(3%), NMC, and NYTG(3%)/NMC samples.

Fig. S2 demonstrated the FT-IR spectra of NYT, NYTG(3%), NMC, and NYTG(3%)/NMC samples. For the NYTG(3%)/NMC sample, the peaks of NYTG(3%) and NMC are all observed indicating that NYTG(3%)/NMC was successfully synthesized. The peak at 1658 cm^{-1} was attributed to the N-H bending vibration of the amino groups in NMC. And the tiny peak at 1340 cm^{-1} corresponds to the C-N stretching on benzene ring. Moreover, the double peaks at 3455 cm^{-1} and 3380 cm^{-1} can be assigned to asymmetric and symmetric vibration of the amino groups in NMC. The peaks at around 2928 and 2855 cm^{-1} corresponding to $-CH_2-$ group and peaks near 1562 and 1464 cm^{-1} corresponding to −COOH group were clearly observed suggesting that the successfully involvement of NYT and NYTG(3%). The introduction of Gd^{3+} ions does not change the infrared peak of upconversion nanoparticles.

Table S1 Photodegradation performance of different upconversion nanoparticles based photocatalysts.

Ln-UCNPs	Coating materials	Light source	Pollutant	Degradation ratio/time (min)	Ref.
$NaYF_4$:Yb,Tm	TiO_2, Fe_3O_4	simulated sunlight	MB	75%/50	1
$NaYF_4$:Gd,Si	TiO_2	simulated sunlight	MB	70%/240	2
BiOBr:Yb,Er 3D Hierarchical Architectures	/	simulated sunlight	RhB	100%/40	3
$NaLuF_4$:Gd,Yb ,Tm@$NaLuF_4$: Gd,Yb	SiO_2, Ag, g-C_3N_4	simulated sunlight	RhB	100%/150	4
$NaYF_4$:Yb,Tm @$NaYF_4$	$Zn_{0.5}Cd_{0.5}S$	simulated sunlight	Cr(VI)	98.7%/30	5
$NaYF_4$:Yb,Tm	TiO_2	simulated sunlight	deoxyniv alenol	90.7%/60	6
$NaYF_4$	SnO_2, Ag	simulated sunlight	RhB	100%/30	7
$NaYF_4$:Yb,Tm, Gd	NH_2-MIL-101(Cr)	simulated sunlight	RhB	79%/90	This work

References

1 Y. Lv, L. Yue, Q. Li, B. Y. Shao, S. Zhao, H. T. Wang, S. J. Wu, Z. J. Wang, Recyclable (Fe_3O_4-$NaYF_4$:Yb,Tm)@TiO_2 nanocomposites with near-infrared enhanced photocatalytic activity, Dalton Trans., 2018, 47, 1666-1673.

2 S. Mavengere, J. S. Kim, UV-visible light photocatalytic properties of $NaYF_4$:(Gd, Si)/TiO_2 composites, Appl. Surf. Sci. 2018, 444, 491-496.

3 Y. J. Li, D. K. Xu, L. Yao, S. H. Yang, Y. L. Zhang, Enhanced upconversion luminescence in controllable self-assembled BiOBr:Yb^{3+}/Er^{3+} 3D hierarchical architectures and their application in NIR photocatalysis, Ind. Eng. Chem. Res. 2018, 57, 17161−17169.

4 F. F. Zhao, K. K. Khaing, D. G. Yin, B. Q. Liu, T. Chen, C. L. Wu, K. X. Huang, L. L. Deng, L. Q. Li, Large enhanced photocatalytic activity of g-C_3N_4 by fabrication of a nanocomposite with introducing upconversion nanocrystal and Ag nanoparticles, RSC Adv., 2018, 8, 42308-42321.

5 W. N. Wang, W. Dong, C. X. Huang, B. Liu, S. Cheng, H. S. Qian, UCNPs@$Zn_{0.5}Cd_{0.5}S$ core-shell and yolk-shell nanostructures: selective synthesis, characterization, and near-infrared-mediated photocatalytic reduction of Cr(VI), J. Nanomater., 2018, 2018, 1-9.

6 S. J. Wu, F. Wang, Q. Li, J. Wang, Y. Zhou, N. Duan, S. Niazi, Z. P. Wang, Photocatalysis and degradation products identifification of deoxynivalenol in wheat using upconversion nanoparticles@TiO_2 composite, Food Chem., 2020, 323, 126823.

7 Q. Y. Tian, W. J. Yao, W. Wu, J. Liu, Z. H. Wu, L. Liu, Z. G. Dai, Efficient UV−Vis-NIR responsive upconversion and plasmonic-enhanced photocatalyst based on lanthanide-doped $NaYF_4$/SnO_2/Ag, ACS Sustain. Chem. Eng. 2017, 5, 10889-10899.